Opposite Page:

Scanning electron micrograph of a patterned layer of amorphous Si, the first step in the process for fabricating the 3-D photonic bandgap structure. (Courtesy of M. Qi)

Optoelectronics

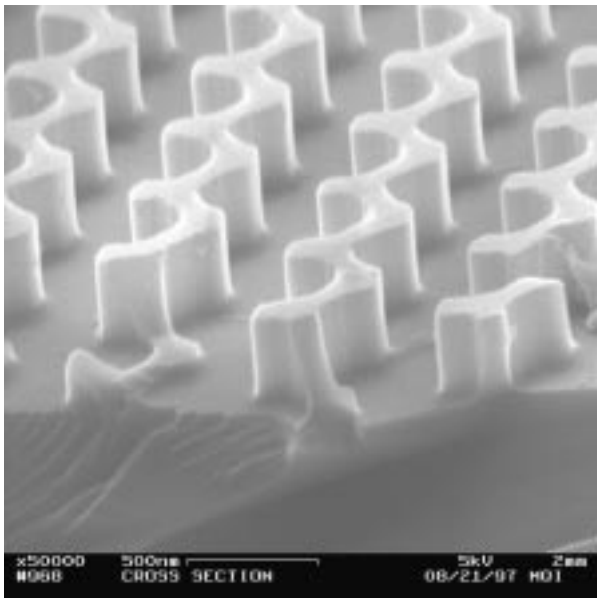

Optoelectronics

- *Development of Semiconductor Optical Devices for All-Optical Communication Networks*
- *Epitaxy on Electronics Integration Technology*
- *InGaAsP/GaAs Light Emitting Diodes Monolithically Integrated on GaAs VLSI Electronics*
- *Low Temperature Growth of Aluminum-Free InGaP/GaAs/InGaAs LED and Laser Diode Heterostructures by Solid Source MBE using a GaP Cell*
- *Dry Etch Technology for Aluminum-free InGaP/GaAs/InGaAs Laser Diode Facets and Deflectors*
- *Development of High Speed Distributed Feedback (DFB) and Distributed-Bragg Semiconductor Lasers*
- *Monolithic Integration of Vertical-Cavity Surface-Emitting Laser Diodes on GaAs VLSI Electronics*
- *Microwave Characterization of Optoelectronic Devices*
- *The OPTOCHIP Project*
- *Monolithic Integration of 1550 nm Photodetectors on GaAs Transimpedance Amplifier Chips*
- *Normal-Incidence Quantum Well Intersubband Photodetectors (QWIPs) for Monolithic Integration*
- *One-Dimensional Photonic-Band-Gap Devices in SOI Waveguides*
- *Photonic Bandgap Structures*
- *Silicon Photonic Band Gap, Microcavity and Waveguide Structures*
- *Three-dimensional Photonic Bandgap Structures*
- *Design and Fabrication of an Integrated Channel-Dropping Filter in InP*
- *Fabrication of an Integrated Optical Grating-Based Matched Filter for Fiber-Optic Communications*
- *Growth of Bandgap-Engineered Distributed Bragg Reflectors*

Development of Semiconductor Optical Devices for All-Optical Communication Networks

Personnel

L. A. Kolodziejski, E. P. Ippen, H. I. Smith, J. G. Fujimoto, H. A. Haus, M. S. Goorsky - University of California, LA, G. S. Petrich, K. L. Hall, G. Steinmeyer, B. E. Bouma, J. N. Damask, E. M. Koontz, J. M. Milikow, S. C. Warnick, I. P. Bilinsky, D. J. Jones, E. R. Thoen, T. E. Murphy, M. J. Khan, M. H. Lim, and K. M. Matney and G. D. U'Ren - University of California, LA

Sponsorship

MIT Lincoln Laboratory and MURI/AFOSR

With the next generation of all-optical networks being designed for operation at speeds of 100 Gbits/sec, the integration of compact, efficient semiconductor-based optical devices offers many advantages. In these high bit-rate networks, low-loss wavelength-selective routing devices and ultrafast optical pulse sources are required.

Waveguide-coupled Bragg-resonant filters provide a compact means of achieving high-density wavelength-selective routing. The functionality of the planar version of these filters is contingent upon the ability to preserve the as-fabricated rectangular-patterned Bragg gratings during the gas source molecular beam epitaxial over-growth; deviations from the rectangular-grating profile result in the inability to selectively route the desired wavelength. Rectangular-patterned gratings, similar in dimension to those required by the Bragg-resonant filters, have been fabricated in both InP and InGaAsP. An *in-situ* low temperature atomic hydrogen-assisted oxide removal technique has been employed to preserve the rectangular grating profile. While the hydrogen-cleaned grating appears to be intact as observed by scanning electron microscopy, the thermally-cleaned grating has experienced profile degradation in the form of rounded grating teeth and filled-in grating trenches.

Triple Axis X-ray Diffractometry (TAD) has been used to provide a nondestructive, high resolution analysis of the overgrown gratings. The (004) TAD reciprocal space maps of InGaAsP deposited on an InP grating reveal the high quality of the InGaAsP epilayer, the presence of a periodic modulation within the overgrown structure as indicated by the existence of satellite reflections and the presence of strain within the structure. The separation of the satellite reflections is related to the period of the grating, and corresponds to an as-fabricated period of 230 nm. The (224) TAD reciprocal space maps confirm that strain is present within the grating region, and is orthorhomically distorting the crystal. The magnitude of the strain is on the order of 10^{-3}, and is expected to have a minimal effect on the optical characteristics of the Bragg-resonant filters.

Currently, passive mode-locking of lasers is the most practical method of generating ultrashort (femtosecond) pulses. Saturable Bragg Reflectors (SBRs) provide a viable means for passive mode-locking a wide variety of solid state lasers. A SBR consists of a saturable absorber (quantum wells within a half-wave layer or a bulk-like epilayer) integrated with a highly reflective mirror [Distributed Bragg Reflector (DBR)]. By epitaxially depositing (via gas source molecular beam epitaxy) the saturable absorber directly on the mirror, the need for additional fabrication steps (i.e. thinning or removing the substrate beneath the saturable absorber and using index matching epoxy to attach a saturable absorber to a commercial mirror) is avoided. Additionally, by selecting the reflectivity of the DBR, the SBR can then be used as either a high reflector or an output coupler in the laser cavity. The SBR structures that have been fabricated to date, contain either two or four InGaAs quantum wells positioned 15 nm from the top of, or centered within, the InP half-wave layer. The DBR contains 22 pairs of quarter-wave AlAs/GaAs layers, resulting in a reflectivity spectrum centered at 1.55 μm. Two SBRs, both with two InGaAs quantum wells positioned 15 nm from the top of the InP half-wave layer, have successfully mode-locked a Cr^{4+}:YAG laser. Since mode-locked fiber lasers offer a number of advantages over other ultrafast sources: compactness, the ability to be pumped with low-power laser diodes, a wavelength of operation centered at the erbium-doped fiber gain peak of 1.55 μm and ease of integration into all-optical fiber networks, SBRs are currently being fabricated for implementation in erbium-doped fiber ring and sigma laser cavities as well as linear fiber cavities containing an erbium/ytterbium co-doped amplifier. ❑

Epitaxy on Electronics Integration Technology

Personnel

J. Ahadian, Y. Royter, S. G. Patterson, and P. T. Viadyananthan
(C. G. Fonstad, Jr., L. A. Kolodziejski, G. Petrich, P. A. Postigo, J. M. Mikkelson, and Dr. W. Goodhue)

Sponsorship

JSEP/RLE, ARPA/NCIPT, NSF, Lincoln Laboratory, and ONR

The development of optical interconnects has been hampered by the lack of a viable source of complex Optoelectronic Integrated Circuits (OIECs), circuits which will ultimately need to contain thousands of optoelectronic devices tightly integrated with VLSI-complexity electronics. Hybriding, wafer-bonding, and epitaxial lift-off have made progress in addressing this need, however issues of density performance, reliability, and yield suggest that monolithic integration is the best answer, as it has been in conventional microelectronics manufacturing. To answer this need we have developed a process, termed Epitaxy-on-Electronics (EoE), for monolithically integrating optoelectronic devices on commercially processed gallium arsenide ICs.

The EoE process begins with custom-designed GaAs VLSI circuits. The electronics technology (the Vitesse Semiconductor HGaAs3 Process) provides enhancement- and depletion-mode MESFETs and four layers of aluminum-based electrical interconnect, as well as Optical Field-Effect Transistor (OPFET) and metal-semiconductor-metal (m-s-m) photodetectors. Molecular Beam Epitaxy (MBE) is used to grow device heterostructures on regions of the GaAs substrate which are exposed by cutting through the interconnect dielectric stack. Established fabrication techniques complete the integration procedure. The unrestricted placement of the optoelectronic devices occurs as part of the routine layout of the integrated circuit; the interconnect dielectric stack in the regions designated for these devices is partially etched at the GaAs foundry forming Dielectric Growth Windows (DGWs). The etch is completed, exposing the underlying GaAs substrate, upon receipt of the ICs from the manufacturer; the design of the DGW structure and of the technique for producing a damage-free GaAs starting surface are among the latest innovations in the EoE process. The source/drain implant is used as the bottom n-contact of the optoelectronic device. Epitaxial material is then grown in the DGWs, while polycrystalline material is deposited on the overglass. Standard processing techniques are then used to remove the polycrystalline material, to fabricate the optoelectronic devices, and to interconnect the top-side electrical contacts of the devices to the electronics.

As in standard silicon technologies, the gallium arsenide VLSI process uses aluminum-based electrical interconnects. We have shown that these interconnects degrade when exposed to temperatures in excess of 475° C. Conventional MBE practice uses a 580° C temperature excursion to desorb the native oxide on the GaAs surface prior to growth, and even this brief high temperature exposure (which was used in previous EoE work) results in appreciable damage to the interconnect lines. Interconnect degradation is now effectively eliminated by using cracked hydrogen to remove the native oxide as low as 350° C.

Also owing to the electrical interconnect thermal instability, the epitaxy must be carried out below 475° C. This restriction is not compatible with the growth of high quality AlGaAs suitable for emitters (although it can be used in passive applications) due to aluminum's high affinity for oxygen. The performance of previous monolithic EoE light emitting diodes involving AlGaAs heterostructures was thus compromised. To circumvent this difficulty, current EoE efforts use the aluminum-free InGaAsP materials system, which is routinely grown a reduced temperatures.

Process innovations in the areas of DGW preparation, low temperature GaAs native oxide removal, and gas-source MBE growth of EoE compatible optoelectronic devices have removed limitations present in previous EoE demonstrations. Ring oscillator measurements made before and after EoE processing have verified stable sub-100 picosecond gate delays, consistent with sub-nanosecond, multi-gigahertz electronics operation. The present EoE technology is now being applied to a variety of applications benefiting from the integration of high performance heterostructure devices with VLSI-complexity electronics. ❑

InGaAsP/GaAs Light Emitting Diodes Monolithically Integrated on GaAs VLSI Electronics

Personnel

P. T. Viadyananthan, J. Ahadian, S. G. Patterson, and Y. Royter
(C. G. Fonstad, Jr., L. A. Kolodziejski, S. Prasad, G. Petrich, and P. A. Postigo)

Sponsorship

DARPA/NCIPT, ONR, and NSF

While surface-emitting lasers are ultimately desired in optical interconnect applications because of their large bandwidth, efficiency, and directionality, recent EoE work has been restricted to the integration of LEDs, with comparatively relaxed growth and fabrication demands, in order to focus attention on the EoE-specific process development. Mesa-confined GaAs/InGaP double-heterostructure LEDs are used in this demonstration of monolithic, emitter-based OEICs.

LEDs are fabricated following epitaxy and removal of the polycrystalline deposits. The fabrication process is nearly identical to that of similar devices on bulk wafers. The primary difference is in the use of thick photoresists (3 to 4 μm) which are needed in order to assure step-coverage over chip-surface non-planarities. Contact lithography is readily used to pattern 2 to 3 μm minimum feature sizes. Step coverage also requires the use of aluminum interconnect metalization. To avoid the undesirable reaction of aluminum with a gold-based ohmic contact, Ti/Pt ohmic contacts are used.

An Al interconnect line links the Ti/Au/Ni p-contact to nearby electronics. An optical shield around the DGW perimeter is formed by stacking interconnect metals up to Metal-3. The purpose of this shield is to prevent coupling of LED emission to nearby electronics. Two shield designs (referred to as #1 and #2) differing in the sizing and placement of metal and via patterns, and consequently differing in surface non-planarity above the shield, were implemented around 50 μm DGWs. Unshielded 85 μm DGWs were also used.

The nominal LED emission wavelength is 873 nm, corresponding to the bandgap of the GaAs core. The angular distribution of the output light is Lambertian, i.e., intensity proportional to the cosine of the normal angle.

Operation of the LED-based OEICs can be illustrated through the example of a simple "optical inverter" on the chip. The input element is an OPFET. With no applied light, the OPFET is in its off state and pulls the output of an inverter loading it to the DCFL high level of 0.6 V. Following three inversions, the signal arrives at the gate of a pull-down EFET as a low. The drain of this off-state EFET rises to 3 V, and 2 V remains across the LED. There is no significant LED current and the optical output is off. When the incident power reaches just above 0.1 μW, the OPFET switches on. The inverter output is now pulled to a DCFL low level of 0.1 V. This signal cascades through the three inverter stages and turns on the pull-down EFET. The drain of this EFET now drops to 0.8 V. With 4.2 V across the LED, the EFET sinks 4.6 mA of current corresponding to an optical output power of 2 μW. This power level is 13 dB above the 0.1 μW optical input threshold. This level of optical gain allows EoE-integrated LED-based OEIC to meet the realistic system requirements of many optical interconnect architectures. In fact, this 13 dB figure represents a lower bound on the optical gain achievable with these OEICs. Use of an 85 μm DGW LED would increase this optical gain to roughly 20 dB. ❑

Low Temperature Growth of Aluminum-Free InGaP/GaAs/InGaAs LED and Laser Diode Heterostructures by Solid Source MBE using a GaP Cell

Personnel
P. A. Postigo
(C. G. Fonstad, Jr. and D. Braddock)

Sponsorship
Lincoln Laboratory

The use of InGaP instead of AlGaAs for the fabrication of light emitting heterostructures as Light Emitting Diodes (LEDs) and Laser Diodes (LDs) presents important advantages, such as the reduction of deep donor levels and lower InGaP/GaAs interface recombination velocity. In addition, InGaP is more suitable for the reduced-temperature Molecular Beam Epitaxy (MBE) required for the Epitaxy-on-Electronics integration technology (475° C), since it is aluminum-free.

The use of phosphorous in MBE has traditionally been done through the introduction of phosphine (PH_3) as a gaseous source. However, the use of a solid source is also very attractive since it is easier to implement and to maintain in the MBE system, but it must be a solid source which gives a very high ratio of dimers to tetramers, i.e., P_2 to P_4 . The dimers have a higher sticking coefficient and are much better for MBE growth. Two methods have been used to produce P_2 from solid sources. One is based in a two-zone-cracker cell where the P_4 is cracked in P_2 by a very high temperature section (>1000° C), and where the source is solid red-phosphorous. The other method is based on the sublimation of phosphorous from phosphides as GaP, which produces the best P_2 to P_4 rate (around 170 compared to the 3.5 to 6 of the thermal cracker). The GaP decomposition cell has the same design as a common group-III effusion cell that operates at high temperatures (the typical temperature used for phosphide growth is around 1000°C) and it can be operated as a regular group-III cell. However, this type of cell can produce some residual amount of Ga, that can be reduced through an special design. This design implements a dome-shaped and disk-shaped Pyrolytic Boron Nitride (PBN) cap on top of the normal crucible, that acts as a trap for the Ga atoms. In collaboration with Dr. David Braddock, from EScience Inc., we have successfully demonstrated a high-capacity (100 gr) GaP decomposition source that has produced high quality epitaxial InP and InGaP. The epilayers have been analyzed by Double-Crystal X-ray Diffraction (DCXR), PhotoLuminescence spectroscopy (PL), and Secondary Ion Mass Spectroscopy (SIMS). The high purity of the P_2 beam obtained through this method and the good behavior of the cell have been used to produce InP/InGaAs photodetectors and InGaP/GaAs/InGaAs LEDs heterostructures at low growth temperature (475° C). Further work will focus on using this P_2 source for reduced-temperature growth of InGaP/GaAs/InGaAs laser diodes for integration on GaAs VLSI chips using the Epitaxy-on-Electronics process. ❑

Dry Etch Technology for Aluminum-free InGaP/GaAs/InGaAs Laser Diode Facets and Deflectors

Personnel

Y. Royter and J. Ahadian
(C. G. Fonstad, Jr., P. A. Postigo, W. Goodhue, and D. Mull)

Sponsorship

Lincoln Laboratory

Aluminum-free InGaAsP/GaAs/InGaAs laser diodes are receiving a great deal of attention currently because of their superior performance and reliability in comparison to more conventional AlGaAs/GaAs/InGaAs laser diodes. Our own interest in these devices is driven by their compatibility with the Epitaxy-on-Electronics (EoE) monolithic optoelectronic integration technology we are developing (described elsewhere in this report). In particular, high quality aluminum-free laser diodes can be grown at temperatures below 475° C, which are compatible with the EoE technology whereas laser diodes with aluminum in or near their active regions can not be grown at such low temperatures.

An important challenge with aluminum-free heterostructures is dry etching vertical end-mirror facets and angled deflector structures, because of the very different chemical make-up of the layers. In particular, the wider bandgap InGaAsP layers contain significant amounts of In and P, and relatively little or no As, whereas the narrow-gap GaAs and InGaAs layers contain roughly 50% As, no P, and relatively little or no In. Conventional chlorine-based and methane-based dry etch techniques do not work well with the aluminum-free heterostructures. We find, for example, that ion-beam assisted chlorine etching of InGaP is very slow at room temperature; at elevated temperatures where the InGaP etches satisfactorily, GaAs layers are etched without the need for the ion beam and severe lateral etching occurs, i.e., the etch is not directional and not anisotropic. While we can make use of this feature in the EoE process for removing polycrystalline deposits, it is not useful for facet etching.

The solution to this problem lies in changing the etchant from chlorine to bromine because the vapor pressures of the relevant bromides are much more similar than are those of the corresponding chlorides. Consequently, it is possible to find etch conditions for which the etch rates of InGaP and GaAs are sufficiently similar that vertical mirror facets can be successfully etched. We have used these results to produce the first etched-facet aluminum-free laser diodes. The threshold current densities of broad-area etched-facet laser diodes are a factor of two higher than adjacent cleaved-facet lasers.

The performance of the current etched-facet lasers is limited primarily by the quality of the etch mask, which we feel is in turn limited by the aligner used. Consequently a 4x projection aligner has been acquired for use on this program and preliminary indications are that its use significantly improves mask quality, i.e., edge definition and smoothness. Future work will combine this new tool with continued work refining the etch chemistry through the combination of both chlorine and bromine in the ion-beam assisted etch system (which is located in MIT's Lincoln Laboratory). A heated, rotatable substrate stage has also been installed on the system in preparation for work on etching curved deflectors. These, along with the vertical end facets, are the key to producing the In-Plane, Surface-Emitting Lasers (IPSELs) we propose to integrate on GaAs integrated circuit chips using the Epitaxy-on-Electronics (EoE) process. ❑

Development of High Speed Distributed Feedback (DFB) and Distributed-Bragg Semiconductor Lasers

Personnel

F. Rana, M. H. Lim, and E. Koontz
(R. Ram, H. I. Smith, and L. Kolodziejski)

Sponsorship

MIT Lincoln Laboratory

High speed semiconductor lasers are becoming increasingly important for high speed optical communication links. With the advent of Wavelength-Division Multiplexing (WDM) technology, single-mode high speed Distributed-FeedBack (DFB) and Distributed-Bragg-Reflector (DBR) lasers are receiving increased attention. These lasers can be directly modulated at frequencies reaching 30 to 40 GHz. Presently, external electro-optic modulators provide the highest modulation bandwidth. However, direct modulation schemes are usually much simpler to implement and integrate. Threfore, any progress made in improving the high frequency performance of semiconductor lasers will have immediate applications in optical communications. The goal of this project is to develop DFB and DBR lasers capable of being modulated at high speeds with low distortion and chirp.

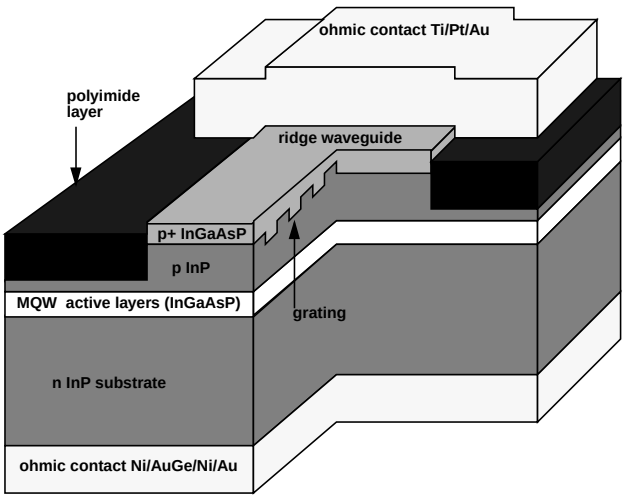

Fig. 1: Polyimide-planarized InP-based DFB ridge-waveguide laser for 1.55 um operation.

High performance DFB and DBR lasers demand careful attention to the design of the grating which provides the optical feedback. Spatial hole burning, side mode suppression, radiation loss, laser linewidth, spontaneous emission in non-lasing modes, lasing wavelength selection and tunability, laser relaxation oscillation frequency are all features that are very sensitive to the grating design. Improved grating design can significantly enhance laser performance, especially at high frequencies. In the last few years various techniques have been developed in the Nanostructures Laboratory that allow fabrication of gratings with spatially varying characteristics and with long-range spatial-phase coherence. Chirped optical gratings with spatially varying coupling parameter can be made using a combination of interferometric lithography, spatially phase-locked electron-beam lithography and X-ray lithography. This provides us a unique opportunity for exploring a wide variety of grating designs for semiconductor DFB and DBR lasers. We plan to explore laser devices suited for high-speed as well as low-noise operation.

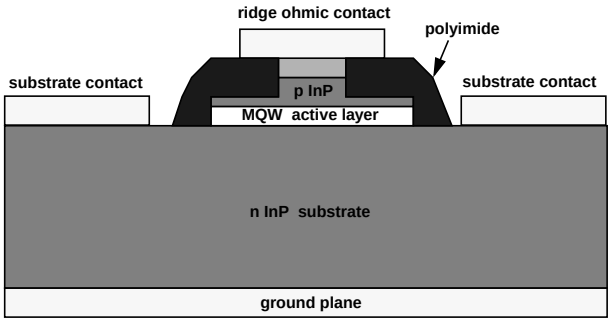

Fig. 2: High speed laser structure with top substrate contact.

continued

continued

We have developed techniques for fabricating high speed polyimide-planarized ridge-waveguide laser structures that have low capacitance and are therefore ideally suited for high frequency operation. A cross section of an InP based DFB laser is shown in Figure 1. The active layers consist of multiple InGaAsP quantum well layers. The grating is etched in InP, and InGaAsP is regrown on top. The ridge is etched and then planarized using polyimide. Ohmic contact to the ridge is made by liftoff on top of the polyimide layer. RC roll off is one of the most important factors that limit the high frequency performance of lasers. The thick layer of polyimide reduces significantly the capacitance between the top metal electrode and the substrate. In addition to this structure, we are also exploring laser structures with co-planar microwave striplines for the ridge and substrate ohmic contacts. This is illustrated in Figure 2. This design offers improved high frequency performance and low series resistance. ❑

Monolithic Integration of Vertical-Cavity Surface-Emitting Laser Diodes on GaAs VLSI Electronics

Personnel

H. Choy
(C. G. Fonstad, Jr. and R. Ram)

Sponsorship

NSF and Lincoln Laboratory

Vertical-Cavity Surface-Emitting Lasers (VCSELs) are particularly suitable as light sources for optoelectronics integration technologies, such as our Epitaxy-on-Electronics (EoE) process. The compact, vertical geometry and the completely epitaxial growth of VCSELs make mass fabrication and testing convenient and economical. The small size of the active region results in low threshold currents. Finally, the surface-emitting property results in an excellent beam profile of the emission, which simplifies coupling to optical fibers. VCSELs are emerging as ideal light emitters for high-density free-space interconnection.

VCSELs consist of several active quantum wells, sandwiched between two highly reflective Distributed Bragg Reflectors (DBRs). These DBRs are realized by epitaxial growth of AlGaAs layers, lattice-matched to GaAs, with varying aluminum and gallium compositions.

The production of VCSELs is not without its own set of challenges. Unlike in-plane semiconductor lasers, light in VCSELs resonates in the direction perpendicular to the thin quantum wells. In order to achieve laser action, the quantum wells must have high radiative efficiency and be situated inside a cavity with a high Q-factor. This requires the DBRs to have very high reflectivities and low total losses; they typically consist of many periods. Several design and growth concerns are important: First, the large number of layers creates numerous heterojunctions which require careful design such that the impedance of the whole device is minimized, and the threshold current and operating voltage remain low. Second, the growth conditions need to be controlled precisely while the structure is being grown, which typically takes four to five hours. Finally, the reflectivities of the top and bottom mirrors need to be carefully designed to strike a balance between high Q-factor and high external efficiency.

continued

continued

Presently, the goal is to achieve flat-bands for carriers in the DBR mirrors as part of the effort to arrive at a low threshold current. This can be achieved by gradually changing the aluminum and gallium compositions with a parabolic profile across the interfaces, while simultaneously maintaining the doping in the span of the grading regions at a much higher level than in the rest of the mirror stack. We focus our effort on p-type top mirrors, since holes have an effective mass eight times more than that of electrons, and thus are much more vulnerable to potential barriers at the heterojunction interfaces.

The optimal design for the grading regions is a compromise between a short enough length and a adequately gradual grading. Short grading regions lower the free carrier absorption resulting from the high doping level and maintain a high overall DBR reflectivity. Gradual grading yields lower impedance mirrors with smaller doping level. The transient behavior of the cells has also to be studied to determine maximum grading speed, because effusion cells used in MBE systems cannot control the flux accurately when the change is too fast.

VCSELs grown on bulk GaAs under normal growth conditions and in-plane lasers with similar quantum wells will be fabricated to compare basic material qualities and growth capabilities. We will also assess the impact of a reduced growth-temperature on the gain of the active region and on the conductivity of the DBR mirrors. This is critical for the adoption of this structure to our EoE technology. ❑

Microwave Characterization of Optoelectronic Devices

Personnel

P. T. Viadyananthan
(C. G. Fonstad, Jr. and S. Prasad)

Sponsorship

DARPA/NCIPT and NSF

The microwave device characterization capability has been expanded so that optoelectronic devices may be characterized using the automatic network analyzer and the on-wafer probe station. The objective was to do a complete characterization of the high speed performance of Light Emitting Diodes (LED's) both discrete and integrated on chip. The aim of e preliminary measurements was to model the high frequency behavior of the LED's and to determine the frequency limits of the desired characteristics. A comparison of the behavior of discrete and integrated devices is important to the understanding of the issues that are unique to the epitaxy-on-electronics integration technology. An accurate estimation of device performance together with physical modeling will result in the efficient application of LED's as emitters in OEIC's and will be the basis of proposed future investigations of high speed surface-emitting lasers.

To this end, measurements were performed on discrete LED's and LED's integrated on the OPTOCHIP. The microwave reflection and transmission properties of the LED's were measured using the HP 8753C network analyzer with a frequency range of 300 kHz to 3 GHz. This range was appropriate for the test devices which operated at frequencies under 3 GHz. The DC bias is applied with an HP 4145B semiconductor parameter analyzer. The optical output from the LED is collected by a high bandwidth detector which is placed close to the emission field of the LED to improve the collection efficiency. A Hamamatsu S5972 p-i-n photodiode with a 3 dB bandwidth of 500 MHz was used as a detector. The electrical signal from the detector was amplified using a high frequency amplifier. The scattering parameters were measured using this experimental arrangement.

continued

continued

Current-voltage (I-V) and light-current (L-I) characteristics were measured initially for a DC analysis. With reverse bias, the bulk devices had a higher leakage current than the integrated devices. It was concluded that lateral confinement was provided by dielectric growth wells in the integrated device on OPTOCHIP. With forward bias, both types of LED's show a turn-on current which is larger than expected. A 4-element model has been proposed to describe these effects The model explains the observed diode characteristics and indicates that the difference in turn on currents is associated with material quality. The difference in efficiencies is due to the different values of the non-radiative recombination coefficient and bimolecular recombination coefficient in the devices measured.

Since the LED is a two terminal device, measurements of S_{21} were used to determine the frequency response. A DC bias was applied to the LED and an RF signal was superimposed with enough RF power for small signal modulation of the LED about the bias level. The bias was varied and the response was measured at each bias level. The frequency response of bulk and integrated devices was measured. The integrated devices on OPTOCHIP had a higher bandwidth than the bulk LED's at comparable bias levels.

Our modeling indicates that the nominally undoped active regions of the LED's was in fact quite n-type, and that significantly higher efficiency and bandwidth will be obtained if the active region is made narrower and is intentionally doped p-type. Such design modifications will be explored to enhance the performance of the LED's. The investigations will then be extended to Vertical Cavity Surface Emitting Lasers (VCSEL's). ❑

The OPTOCHIP Project

Personnel

J. Ahadian, S. G. Patterson, P. T. Viadyananthan, and Y. Royter (C. G. Fonstad, Jr., L. A. Kolodziejski, G. Petrich, P. A. Postigo, and J. M. Mikkelson)

Sponsorship

DARPA/NCIPT and ONR

The OPTOCHIP Project is a research foundry offering intended to provide prototype OEICs to selected university groups doing research on optical interconnect systems. The first generation OPTOCHIPs use InGaP/GaAs Light Emitting Diodes (LEDs) monolithically integrated using the Epitaxy-on-Electronics (EoE) technology on commercially fabricated GaAs integrated circuit chips containing OPtical Field Effect Transistor (OPFET) and Metal-Semiconductor-Metal (m-s-m) photodetectors, and enhancement- and depletion-mode metal-semiconductor field effect transistors (MESFETs). A solicitation for participation was made in late 1995 and in early 1996 nine groups from eight universities were selected to participate; the universities represented are California Institute of Technology, Colorado State University, George Mason University, McGill University, Texas Christian University, University of Southern California, and University of Washington. These groups began work in February 1996 on the designs for 2 mm by 2 mm OEIC chips which were combined into a larger die and submitted to the MOSIS service in May 1996. The chips were fabricated by Vitesse Semiconductor Corporation, Camarillo, CA, in the summer and fall of 1996, and the EoE integration process was initiated early in 1997. Fabrication of the integrated LEDs was completed in May 1997, and the completed OPTOCHIP die were sewn into individual 2 mm by 2 mm chips and returned to the designers for deployment in their optical interconnect architectures.

Electrical tests on the completed OPTOCHIP die show that there was no degradation in the electrical performance of the circuitry due to the EoE process. The performance and yield of the LEDs were poorer than had been achieved on previous test runs, due it appears to problems in the growth system, but several functional die were provided to each participating group. The amount of work done with the completed chips varies between the various groups, but several groups have performed extensive testing of their OEIC chips and have

continued

continued

successfully employed them in systems-level situations. In one case, communication between a pair of OPTOCHIPs has been demonstrated. Work is continuing on the testing of the chips, and our group at MIT is working to be able to supply the participants with another set of die processed using the new GaP phosphorous source recently installed on our MBE.

The completed, overall 7 mm by 7 mm square OPTOCHIP die each contain over 200 LEDs integrated with numerous different circuits and subsystems containing thousands of transistors. As such they represent some of the most complex LED-based monolithic OEICs ever fabricated. The OPTOCHIP project was also unique in that the OPTOCHIP die incorporate designs from a diverse selection of groups and in that minimal constraints were placed on the circuit designs.

Our intention is that there will be future OPTOCHIP offerings, and that the processing of subsequent OPTOCHIPs will be done on a semi-professional basis using the facilities of the Technology Research Laboratory (TRL) of the Microsystems Technology Laboratory (MTL) at MIT. We are anxious to make Surface-Emitting Lasers (SELs) available to OPTOCHIP users in the near future; Self-Electro-optic Effect Devices (SEEDs) are another option, but our primary focus is on emitter-based OEICs containing LEDs or SELs. ❑

Monolithic Integration of 1550 nm Photodetectors on GaAs Transimpedance Amplifier Chips

Personnel

H. Wang
(C. G. Fonstad, Jr., R. Hemenway, R. Deming, and J. Mikkelson)

Sponsorship

MIT Lincoln Laboratory

High data rate optical communication systems require increasingly complex integration of high performance electronic circuits with sophisticated optoelectronic devices. In the short run these needs can be met by hybrid assemblies. However the cost, performance compromises, and reliability concerns associated with hybrid integration, and the increasing need for specialized subcircuits which are not commercially available, make development of the monolithic integrated circuit technology extremely desirable.

We are using several techniques to monolithically integrate 1550 nm photodetectors with Gallium Arsenide (GaAs) TransImpedance Amplifiers (TIAs) to form monolithic OptoElectronic Integrated Circuits (OEICs) for fiber-based systems. Both Epitaxy-on-Electronics (EoE), described elsewhere in this report, and selective area semiconductor wafer bonding, also described elsewhere in this report, will be utilized. In the EoE process, optical devices are epitaxially grown on fully processed GaAs integrated circuits. For this application, high-speed photodetectors based on the lattice-mismatched InGaAs/GaAs material system are being developed and evaluated. For the wafer bonding process, fully lattice-matched photodetector heterostructures, grown under optimal conditions on InP, will be bonded onto the same GaAs circuits. After EoE epitaxy or wafer bonding, the device heterostructures will be processed and monolithically integrated with the pre-existing electronics, yielding high speed, compact, reliable monolithic OEIC'S.

The GaAs transimpedance amplifier test chip (MIT-OEIC5/LL-MORX1), which incorporates modified versions of a commercial Vitesse transimpedance amplifier, has been designed and submitted to MOSIS for processing. Included on this chip are polarization diversity heterodyne photoreceivers, dual-balanced photoreceivers, and other functional cells; the chip is which are suitable for both EoE epitaxy and wafer bonding.

continued

continued

Initial results from measurements on 1550 nm photodiodes grown on GaAs have been obtained. The performance of $In_{0.52}Al_{0.48}As/In_{0.53}Ga_{0.47}As$ pin photodiodes grown on GaAs substrates using linearly graded buffers were compared with those using graded short-period superlattice (GSSL) buffers. Detectors on linearly-graded buffer are found to be superior to those on GSSL buffer. However, the best dark current levels seen (5 μA for 50 μm square detectors at 2V bias) must to be reduced for final integration.

Several approaches to the reducing the leakage are being investigated simultaneously. A side-wall passivation technique using polyimide has been proposed and the required mask set is being generated. A second method is to replace the wide gap InAlAs with electrically superior InP. New heterostructures using InP as cladding layers have been grown and are being processed. Thirdly, we have lowered the indium concentration grading rate from 17% per micron to 10% per micron, aiming at lowering threading dislocation density in the absorption layer. Finally, a novel structure, the Uni-Travelling-Carrier Photodiode (UTC-PD), is being considered for both dark current reduction and speed enhancement.

Optimized detector MBE growths have been carried out on both n-GaAs and n-InP substrates for a comparative study of the effects of lattice mismatch. Photodetectors will also be grown on p-InP substrates in order to be bond onto the GaAs chips. Wafer bonding using both direct bonding of InP and InGaAs to GaAs by atomic rearrangement, and bonding with palladium assistance will be investigated. The method yielding the best electrical characteristics will be chosen to bond the detectors onto OEIC5 chips.

Future work will expand the effort to include integration of 1550 nm light emitters as well as detectors, which requires significant work on direct wafer bonding of InP-based materials onto GaAs chips and/or work on high quality lattice-mismatched InGaAs/InP epi-layers on GaAs. ❑

Normal-Incidence Quantum Well Intersubband Photodetectors (QWIPs) for Monolithic Integration

Personnel

J. Pan
(C. G. Fonstad, Jr.)

Sponsorship

NSF, ONR, and Lockheed-Martin

Band gap engineering allows us to design the peak responsivity of a Quantum Well Intersubband Photodetector (QWIP) to be at anywhere in the infrared region beyond about 2 μm. This wavelength region is useful for spectroscopy and identification of unknown gases, as well as for imaging in the Earth's atmosphere in the transparent spectral regions of 3 to 5 μm and 8 to 12 μm. The narrow spectral responsivity of QWIPs allows for the use of lenses, which are cheaper and smaller than mirrors, in the optical systems used to focus infrared radiation onto the detectors. This flexibility in the location of the peak in the responsivity spectrum, as well as the narrow spectral width of the responsivity, are also useful in he design of dual band and dual color QWIPs. Detection of the infrared radiation emanating from an object at two different wavelengths makes it possible to ascertain the absolute temperature of the object and to distinguish it from the "clutter" surrounding it.

Modern epitaxy techniques can achieve high uniformity of semiconductor parameters across entire III-V (GaAs and InP) wafers, which allows for the realization of large Focal Plane Arrays (FPAs) of QWIPs with low spatial (fixed) pattern noise. Furthermore, the growth of QWIPs on GaAs substrates is compatible with the monolithic integration of QWIPs with standard GaAs detector circuits. Monolithic integration would remove the need for indium bump bonding, an extra processing step which contributes to increased expense and reduced yield, and monolithic integration is one of the important objectives of our program. Specifically, our goal is to fabricate QWIPs which can be monolithically integrated with standard GaAs detector circuits using the Epitaxy-on-Electronics (EoE) process.

QWIPs which can respond to normally incident radiation will eliminate the need for an optical grating and for thinning of the devices, thus simplifying the processing and increasing the processing yield for such devices. However, the intersubband absorption of normally

continued

continued

incident radiation is in general very weak; it depends on the size of the electron's transverse wave vector or the size of the bulk spin-orbit interaction. By paying special attention to such issues we have successfully demonstrated the first n-type QWIP (n-QWIP) which responds to normally incident radiation without the use of an optical grating. Such QWIPs are observed to have a conversion efficiency of about 3%. While this is an important result, the quantum efficiency of such devices can be increased further by utilizing a transition which exhibits even stronger absorption of normally incident radiation. We are currently investigating strained, pseudomorphic p-type QWIPs for this purpose.

Whereas tactical missions in the past have required focal plane arrays to detect targets which are brighter than the background, with about 10^{16} photons/cm^2-s reaching the detector, recently, there has been a shift in the applications of quantum well infrared photodetectors towards detection in space of faint targets at large distances of several thousand kilometers with only about 10^{13} photons/cm^2-s reaching the detectors. Future work on QWIPs must not only focus on increasing the photoconductor conversion efficiency, but also on the more stringent requirements on FPA uniformity, linearity, and dark current of such applications. Faint targets require larger pixel sizes and better uniformity across the fewer pixels. Better linearity is also needed in situations where absolute radiometry is required. Device modeling is now being carried out in an effort to increase the ratio of the photocurrent to the dark current by increasing the ratio of the photoconductive gain to dark current gain. ❑

One-Dimensional Photonic-Band-Gap Devices in SOI Waveguides

Personnel

S. Fan, J. Ferrera, J. S. Foresi, G. Steinmeyer, E. R. Thoen, and P. R. Villeneuve (E. P. Ippen, J. D. Joannopoulos, L. C. Kimerling, and H. I. Smith)

Sponsorship

NSF and JSEP

Photonic Band Gap (PBG) structures are optical analogs of semiconductors. A light wave traveling through a PBG structure encounters a large, periodic change in the dielectric constant. The periodicity causes bands of frequencies to be disallowed from propagating through the structure. These bands can be as large as 30 percent of the mid-gap frequency. PBG's can be designed in 1-, 2-, and 3-dimensions. 1-D PBG's are similar to distributed Bragg reflectors (DBR's), but have much larger gaps; band gaps for DBR's are typically less than 1 percent. In this project we have developed 1-D PBG's that are directly integrated into silicon waveguides. Their band gaps are centered at $\lambda = 1.54$ μm. This wavelength is compatible with commercial fiber optic communication systems.

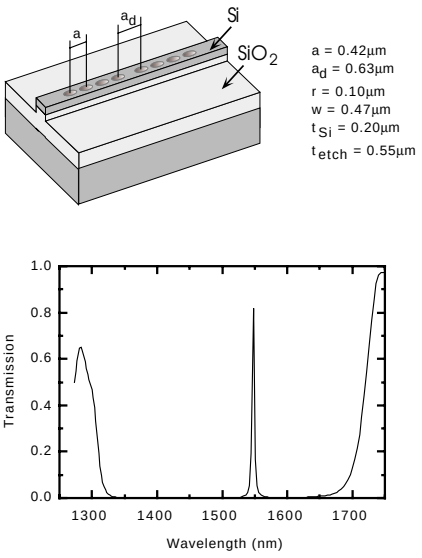

Fig. 3: Dimensions and basic properties of a PBG microcavity. a) Schematic of a PBG waveguide microcavity with dimensions for operation at $\lambda = 1.54$ μm: a is the hole period, a_d is the defect length, r is the hole radius, w is the waveguide width, t_{Si} is the silicon thickness and t_{etch} is the total etch depth through both the Si and the oxide. b) Computation of the transmission through the structure. The transmission spectrum corresponds to the device dimensions listed. The resonance is centered at 1.547 μm and has a Q of 280.

continued

continued

We have fabricated and measured a 1-D PBG microcavity with a resonance at $\lambda = 1.56$ μm, a quality factor (Q) of 265 and a modal volume (V) of 0.055 μm^3, which makes it the most tightly confined photon mode ever achieved. Its applications range from the control of spontaneous emission in light emitting materials, to channel dropping filters for wavelength division multiplexing.

The 1-D PBG device consists of a single-mode strip waveguide fabricated from SOI material with a periodic series of holes etched through the Si (Figure 3). The large dielectric contrast between the Si and the holes (12:1) results in a band gap of 27 percent of the mid-gap frequency. The waveguide width is approximately 0.47 μm, with holes of 0.20 μm diameter, separated by 0.42 μm, center to center. The minimum dimension, 0.13 μm, occurs between the edges of the waveguide and the edges of the holes. Because of the small feature size we use a combination of e-beam and X-ray lithography for patterning. To minimize possible alignment errors, we fabricated an X-ray mask that contained both the waveguide and hole structures. The holes were etched into long waveguides (typically around 2 mm) which required stringent control of e-beam field stitching.

The device, which consists of two sections of four holes separated by a gap, behaves as a microcavity. Light gets localized in the region between the two sets of holes. The holes act as mirrors, forming a resonant cavity within the waveguide. The transmission spectrum of this structure was computed using a three- dimensional finite-difference time-domain method.

The devices were fabricated from a Unibond silicon-on-insulator substrate with a 0.2 μm single-crystal silicon layer on a 1.0 μm oxide layer. The relatively thick oxide is required to keep the optical mode of the waveguide from leaking into the substrate. The wafer was then coated with PMMA and the pattern transferred to the PMMA via X-ray lithography. The PMMA was developed and a 50 nm Cr layer evaporated onto the sample. The PMMA was then dissolved in acetone, leaving intact the Cr which was in direct contact with the Si. The Si layer was then etched in a CF_4 plasma with 15 percent O2. An additional etch into the oxide was performed using CHF_3. The oxide etch was shown theoretically to improve the performance of the PBG device.

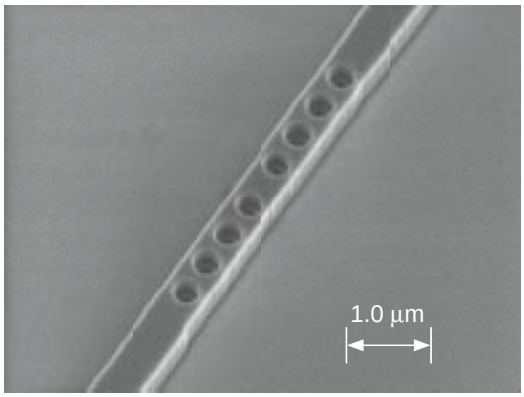

Fig. 4: Scanning electron micrograph of a 1-D photonic-bandgap microcavity in Si on SiO_2, fabricated using e-beam and X-ray lithographies, Cr liftoff, and reactive ion etching.

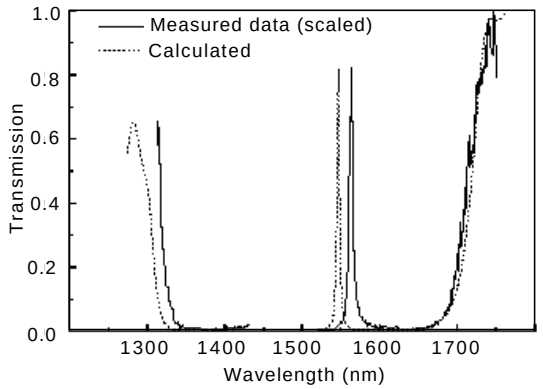

Fig. 5: Comparison of measured transmission (solid lines) to calculated transmission (dotted line) for a PBG microcavity with four holes on each side of the microcavity.

continued

continued

A scanning electron micrograph of a completed PBG waveguide device is shown in Figure 4.

The transmission through the device was measured by coupling light from a tunable color-center laser, with a wavelength range from 1.500 μm to 1.625 μm. The ratio of transmitted to incident intensity was then measured as a function of wavelength. Figure 5 shows the measured (solid) and calculated (dotted) transmission spectra for this microcavity. A resonance is seen at $\lambda = 1.560$ μm, which is within 1% of the calculated resonant wavelength of 1.547 μm. The measured Q is 265, while the calculated Q is 280. The measured values are in remarkable agreement with theory. ❑

Photonic Bandgap Structures

Personnel

L. A. Kolodziejski, J. D. Joannopoulos, E. P. Ippen, H. I. Smith, G. S. Petrich, S. Fan, P. Villeneuve, G. Steinmeyer, K.-Y. Lim, and D. J. Ripin

Sponsorship

NSF/MRSEC

This project represents the combined effort of the research groups led by Professors J. D. Joannopoulos, L. A. Kolodziejski, E. P. Ippen, and H. I. Smith. Prof. Joannopoulos' research group designs the structures and theoretically calculates the optical properties. Prof. Kolodziejski's group fabricates various devices exhibiting photonic band structures in one-, two- and three-dimensions using III-V compound semiconductor technologies. Prof. Smith's group provides the expertise in nanoscale fabrication. Finally, the devices are optically characterized by Prof. Ippen's research group. The complexity of the design, fabrication and characterization of these structures necessitates a strong interaction between the various research groups.

A photonic crystal is a periodic dielectric structure that prevents photons within a certain range of frequencies from propagating. This forbidden band of frequencies translates into a Photonic BandGap (PBG). A defect state can also be introduced in the photonic bandgap when the selective removal or addition of dielectric material breaks the dielectric periodicity of a photonic crystal. This defect results in the spatial localization of the defect mode into a volume of approximately one cubic wavelength, yielding a high-Q electromagnetic microcavity which promises to vastly reduce the spontaneous emission and zero point fluctuations within an energy band. The realization of such a microcavity holds the promise of vastly reducing the spontaneous emission and zero point fluctuations within an energy band.

One, two- and three-dimensional PBG structures are being fabricated. In the one-dimensional monorail microcavity, the photonic crystal consists of a GaAs waveguide containing an array of holes that are etched through the waveguide. The waveguide itself resides on a layer of Al_xO_y which has a much lower refractive index than GaAs. In the one-dimensional air-bridge microcavity, the microcavity consists of a GaAs waveguide with a series of holes etched into the

continued

continued

Silicon Photonic Band Gap, Microcavity and Waveguide Structures

Personnel

J. Foresi, T. Chen, K. Chen, and D. Lim
(L. C. Kimerling)

Sponsorship

NSF/MRSEC

waveguide that is suspended in air, thus resulting in a higher index contrast between the photonic crystal and its surroundings. Both the monorail and air-bridge microcavity devices are designed to operate at the technologically important wavelength of 1.55 μm and have waveguides coupled into and out of the devices to facilitate the optical characterization of these devices. A two-dimensional photonic bandgap effect is being used to enhance the extraction efficiency of a Light Emitting Diode (LED). In particular, the device consists of a LED structure with a periodic series of holes etched into the active layer. The presence of the photonic crystal inhibits guided modes in the active layer and hence, the only allowed modes for the light to couple into are the radiation modes. This translates to a higher flux of radiation emitted in the vertical directions. The LEDs have been grown and are currently being processed. The three dimensional PBG structure consists essentially of two interpenetrating DBRs composed of GaAs and Al_xO_y in which a series of holes are etched at normal incidence through the top surface of the structure. By first etching a grating into a GaAs/AlAs DBR and then by regrowing the second GaAs/AlAs DBR within the trenches of the grating, a periodic structure of GaAs and AlAs can be formed both normal to and parallel to the surface. After the regrowth procedure, a series of holes will be etched into the structure and the AlAs will be oxidized to form Al_xO_y, creating a three-dimensional photonic crystal. Currently, the grating is being etched into the first GaAs/AlAs DBR.

The Microsystems Technology Laboratory, the Nanostructures Laboratory and the Building 13 Microelectronics Fabrication Laboratory are being used to fabricate the PBG structures. The initial compound semiconductor material for the photonic bandgap structures is grown by gas-source molecular beam epitaxy in the Chemical Beam Epitaxy Laboratory. ❑

Photonic Band Gap (PBG) devices are optical analogs of semiconductors. A lightwave traveling through a PBG structure encounters a large, periodic change in the dielectric constant. This periodicity causes bands of frequencies to be disallowed from propagating through the device. In this project we have developed 1-D PBG's that are directly integrated into silicon waveguides. Their band gap is centered at $\lambda = 1.54$ μm. This wavelength is compatible with fiber optic communication systems. Our contribution to this program is in collaboration with Professors Haus, Ippen, Kolodziejski, and Smith (EECS), and Professor Joannopoulos (Physics). The 1-D PBG device consists of a single mode, strip waveguide fabricated from SOI material with a periodic series of holes etched through the Si. The large dielectric contrast between the Si and the holes results in a band gap of 15% of the mid-gap frequency. The waveguide width is approximately 0.55 μm, with holes of 0.3 μm diameter, spaced at 0.48 μm. The minimum dimensions for these structures, 0.1 μm, occurs between the holes, and between the edge of the waveguide and the edge of the holes. This small feature size necessitates the use of l.c. X-ray lithography for patterning. To minimize the possible alignment errors, we fabricated an l.c. X-ray mask that contained both the waveguide structure and the hole structures together. E-beam writing these long (typically 2 μm) waveguide devices require stringent control of field stitching to eliminate stitching errors. We have demonstrated the world's first 1D photonic band gap structure at an optical wavelength. The measured Q was 265, at a center frequency of 1564 nm and a modal volume of .055 μm^3.

continued

continued

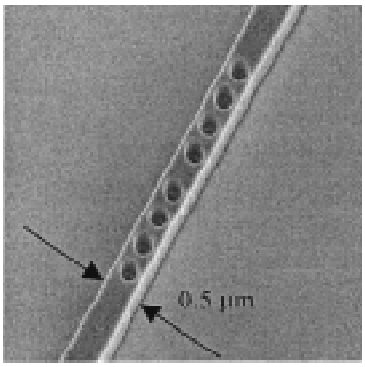

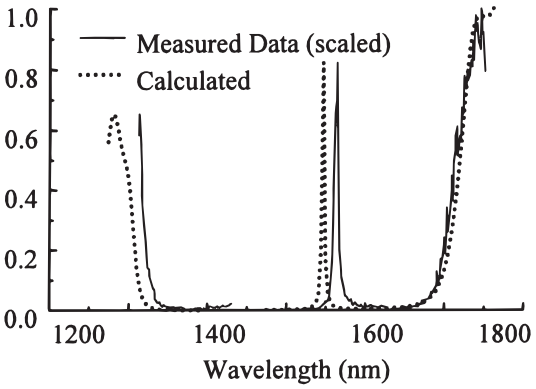

Fig. 6: (left) SEM photograph of 0.5 μm wide PBG waveguide with 4 holes on either side of a small cavity. (right) Transmission versus wavelength for the pictured structure. The resonance of the cavity is at ~1565 nm.

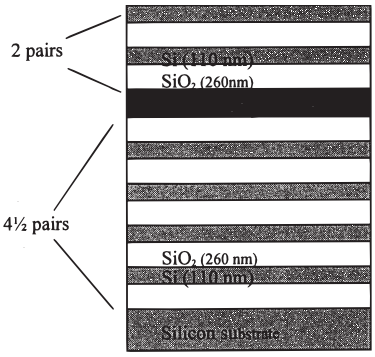

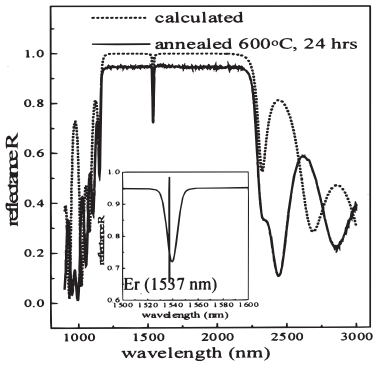

Fig. 7: (left) Si/SiO_2 microcavity with Si:Er active layer. The cavity has an active layer that is tuned for 1537 nm. (right) Reflectance spectrum of microcavity with resonance at 1537 nm. The cavity quality factor is ~300. (fabricated at Polaroid-Norwood).

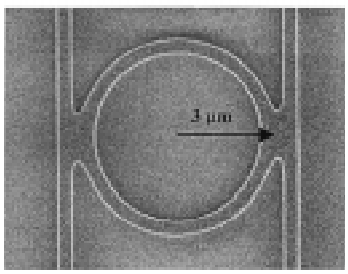

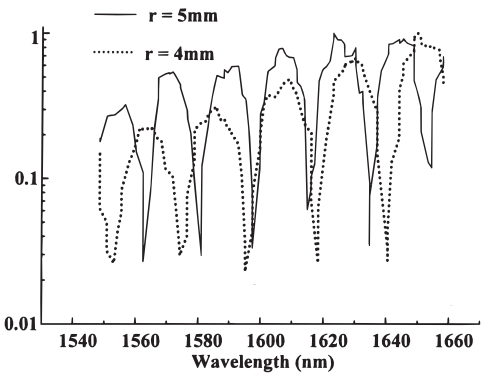

Fig. 8: (left) SEM photograph of ring resonator with fused waveguides (fabricated at HP). (right) Normalized transmission versus wavelenght for rings of radii 4 and 5 μm.

continued

continued

Novel microring resonator structures have also been designed, fabricated, and demonstrated. Resonances with Qs of 250 were observed at $\lambda = 1.55$ μm. These structures are candidates for large scale, integrated add-drop filters for WDM networks. By engineering the poly-Si waveguide fabrication process to reduce losses by light scattering and absorption, we have achieved a world record transmission loss of 9 dB/cm at $\lambda = 1.54$ μm. These structures and level of performance are the first to meet the requirements for on-chip, optical clock distribution. The main sources of loss are light scattering by rough surfaces and absorption at dangling bond-sites. ❑

Three-dimensional Photonic Bandgap Structures

Personnel

M. Qi
(J. D. Joannopoulos and H. I. Smith)

Sponsorship

NSF

In order to achieve a photonic bandgap in three dimensions, the structure must present a periodic modulation of the refractive index in three dimensions. Moreover, that modulation must be of a specific form. To date, two specific types of periodic modulation have been found that theoretically enable a true bandgap for all possible directions of propogation. One of them, illustrated in Figure 6, is designed to enable the use of planar fabrication techniques.

The objective of this project is to fabricate the structure illustrated in Figure 9 by means of a multi-step process consisting of: amorphous-Si deposition; lithography and etching of the Si; depostion and planarization of thick SiO_2 ; reactive-ion etch back of the SiO_2 to the level of the Si; and then a repeat of this sequence until about 7 layers are achieved. In between successive layers, a critical alignment step is required, as can be seen from Figure 9. Theoretical analysis has shown that 7 layers are sufficient to achieve a 3-D bandgap.

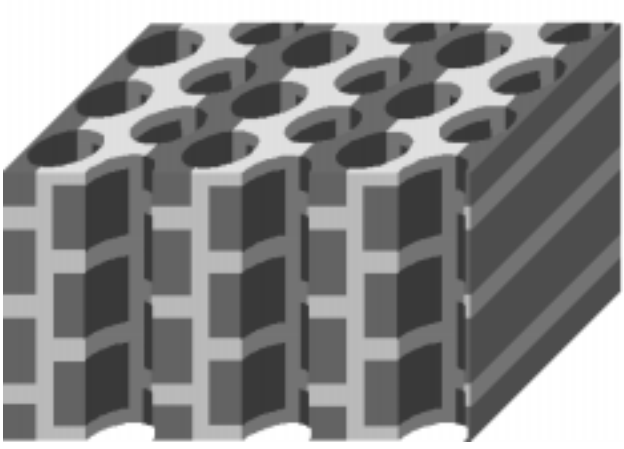

Fig. 9: Depiction of a 3-D photonic-bandgap crystal to be fabricated at a 790 nm period. The dark gray and light gray regions correspond to Si, with a high refractive index (3.4) and SiO_2, with low index (1.4), respectively.

continued

continued

Our approach to date has been to use Scanning-Electron-BeamLithography (SEBL) because of its flexibility, the ease with which design changes can be made, and its ability to perform the precision alignment. SEBL restricts us to relatively small areas because of the slow writing time and problems due to drift of the beam location. However, for an initial demonstration small areas are sufficient. If larger areas are required in the future, X-ray lithography could be employed.

Figure 10 illustrates an etched amorphous Si layer, the first step in the process for fabricating 7-layer, 3-D photonic-bandgap structures. The lithography is done in the NSL's scanning-electron-beam lithography system, and the etching is done by reactive-ion etching in CF_4/O_2. ❑

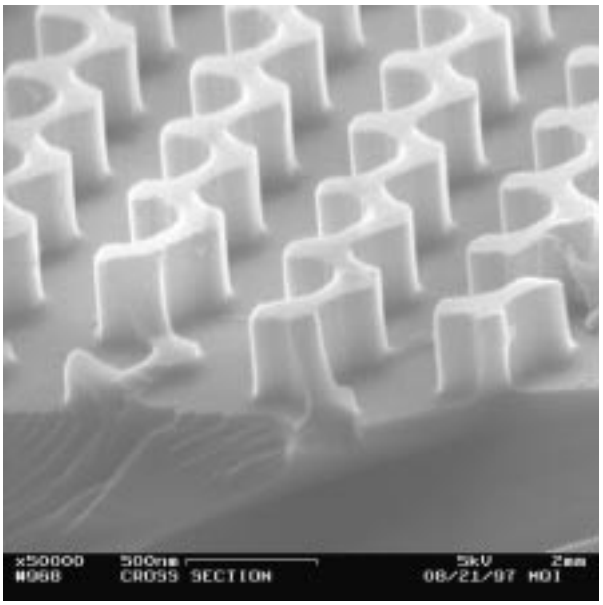

Fig. 10: Scanning electron micrograph of a patterned layer of amorphous Si, the first step in the process for fabricating the 3-D photonic bandgap structure illustrated in Figure 9.

Design and Fabrication of an Integrated Channel-Dropping Filter in InP

Personnel

J. N. Damask, M. H. Lim, J. Ferrera, M. J. Khan, E. M. Koontz, T. E. Murphy, L. A. Kolodziejski, H. A. Haus, and H. I. Smith

Sponsorship

DARPA and AFOSR

In order to meet the ever-growing demand for telecommunications, it will be necessary to exploit the enormous capacity offered by optical communications. Wavelength Division Multiplexing (WDM) is one way to utilize more of the available bandwidth in optical communications by transmitting several distinct communications channels on one optical fiber, each channel at a different wavelength within the communications band (analogous to AM/FM radio transmission.) This technology relies on optical filters to distinguish between the various channels. The channel dropping filter which we are building at MIT is one such device. Its function is to selectively add or drop a single communication channel from an optical communication stream without affecting the remaining channels.

Figure 11 is a sketch of our most recent design of the channel-dropping filter. The bus waveguide carries many communication channels, each centered at a different wavelength. The filtering operation is performed by the quarter-wave-shifted resonators, located on either side of the bus waveguide. The Bragg grating structure, containing an abrupt quarter-wave phase shift in the center acts as an optical resonator which is excited only by a specific wavelength. The resonant wavelength is tapped off into the upper waveguide of the device, while all other wavelength channels continue along the bus undisturbed. Figure 11 also illustrates the calculated spectral response of the device. Note that the device may also be used in the reverse manner, *i.e.*, to inject or add a specific wavelength channel.

Figure 12 illustrates the waveguide structure of the channel-dropping filter. The device is built on an InP substrate, with a quaternary InGaAsP core material. After the waveguide core and Bragg gratings are patterned lithographically, a final layer of InP cladding (not depicted in Figure 12) is deposited over the top of the structure, thereby creating a channel waveguide. In order for the device to operate within the 1.55 μm

continued

continued

communications band, the Bragg-grating period must be approximately 240 nm. Constructing the device in InP offers the potential for integration with other optoelectronic components of the communications system, such as detectors or DFB lasers. Moreover, although the channel dropping filter described here is a passive device, the properties of InP could be later exploited to build related active devices.

The curved-bus depicted in Figure 11 represents a significant improvement in the channel dropping filter design. Previous designs called for a straight bus waveguide, but we have found that by curving the bus towards and away from the resonators, it is possible to reduce the crosstalk level outside of the grating stop-band. It is important that those channels located far from the center-wavelength of the filter not be transmitted into the upper waveguide along with the dropped channel. Previous straight-bus designs were found to transmit a large fraction of power outside of the grating stop-band into the upper waveguide. Thus, for the straight-bus devices, the number of usable wavelength channels was limited by how many could fit within the grating stopband. The improved curved-bus design helps to ease this constraint by reducing the out-of-band transmission. Moreover, the curved-bus design is predicted to be more tolerant of fabrication errors .

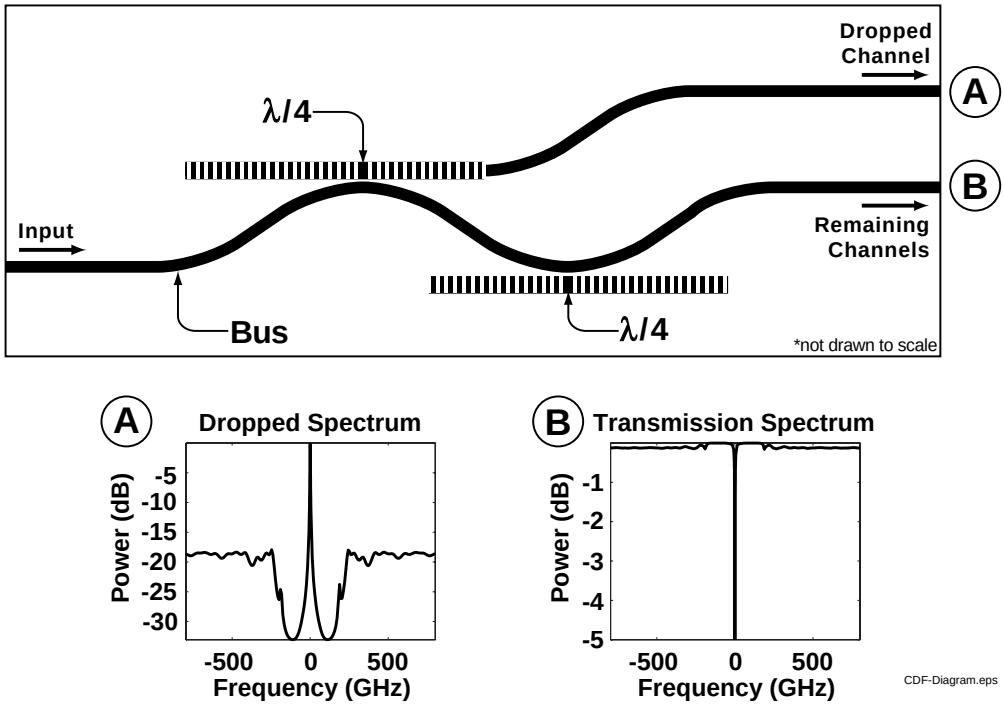

Fig. 11: Diagram of the channel-dropping filter design. Several wavelength channels propagate along the bus waveguide, and one particular channel is tapped off into the upper waveguide.

continued

Because the grating period required for the channel dropping filter is ~240 nm, high-resolution nanolithography techniques are required to pattern the Bragg gratings. A further requirement is that the grating patterns be spatially coherent over lengths of several hundred microns. This means that there cannot be any phase errors or stitching errors in the written gratings, something which cannot be achieved with conventional e-beam lithography. We use a technique called spatial-phase-locked e-beam lithography to write the grating patterns onto an X-ray mask. X-ray nanolithography is then used to transfer the fine-period patterns repeatably onto the InP substrates. Spatial-Phase-Locked E-Beam Lithography (SPLEBL) uses an interferometrically generated fiducial reference grating on the X-ray mask to ensure that there are no phase errors (or stitching errors) when writing the grating resonators. One significant challenge to building the channel-dropping filter is to precisely fabricate a specified grating frequency. The center-frequency of a filter is determined by the period of the grating and the material index of refraction. If the fabricated grating period is uncertain to 1 nm, the center frequency of the filter could be off by as much as 800 GHz, which would make the filter completely miss the desired channel. We have developed a novel interferometric lithography system which allows us to repeatably control grating periods to well within 1 nm.

It is crucial to the operation of the channel-dropping filter that the bus waveguide and resonators be synchronous. This means that at the center-frequency of the filter the propagation constants of the two waveguides depicted in Figure 12 must be equal . This translates into tight tolerances on the waveguide and grating geometry. It is therefore important that all lithography steps be carefully characterized and controlled. Additionally, when the final cladding layer of InP is deposited over the top of the device, it is important that the waveguide and grating structures not be disturbed. To this end, we have developed and demonstrated III-V deposition techniques which can be used to deposit material over fine-period gratings without appreciably effecting the shape of the underlying grating structure. The design of the channel-dropping filter has been completed and most of the fabrication steps have been developed and characterized. We are presently in the process of integrating all of the process steps. ❑

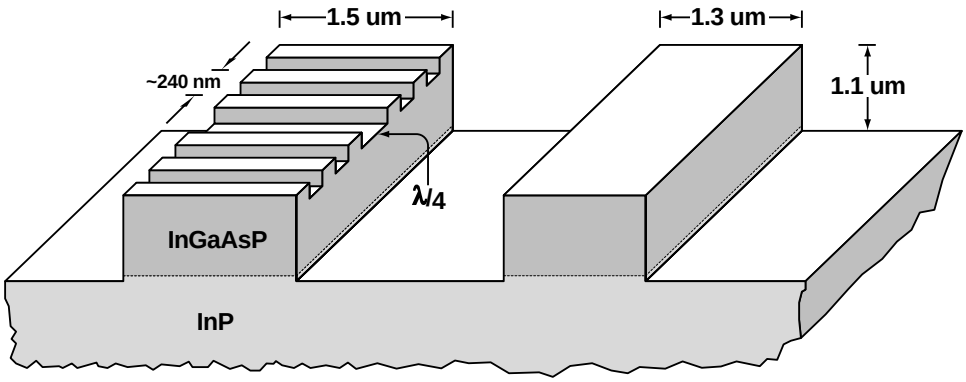

Fig. 12: Waveguide structure of the channel-dropping filter. A grating of ~240 nm period is etched into the top surface of the resonator waveguide. After all lithography steps are performed, a final layer of InP cladding (not depicted) is deposited over the structure.

Fabrication of an Integrated Optical Grating-Based Matched Filter for Fiber-Optic Communications

Personnel

J. N. Damask, T. E. Murphy, M. H. Lim, and J. Ferrera
(H. I. Smith)

Sponsorship

DARPA and AFOSR

For future all-optical communication systems, filters are needed for a wide variety of network functions including dispersion compensation, wavelength multiplexing, gain flattening, and noise suppression. This project seeks to develop the technology for building such filters, using integrated Bragg gratings. Integrated gratings provide a convenient way to perform filtering operations, in a package that can be integrated on a chip with other electronic and optical components of the communications system. As a vehicle for demonstrating this technology, we are in the process of fabricating an integrated matched-filter. The matched-filter is a grating-based device designed to filter out unwanted noise from an optical communication signal.

The dominant source of noise in most modern communications systems is the broad-band noise generated by amplified spontaneous emission in optical amplifiers. A filter is needed in order to separate the communication signal of interest from this unwanted background noise. Because the broad-band noise typically overlaps with the signal of interest, the most suitable filter is one that has a spectral response similar in shape to the signal. The goal of our project is to build a matched-filter, i.e. a filter with a spectral response that is matched to the communications signal. Such a filter is predicted to yield better performance than currently-used Lorentzian filters. Moreover, because the filtering is performed with an integrated Bragg grating, the device has the potential of being integrated with other components of the optical receiver.

One of the most common methods of encoding binary information on an optical signal is to modulate the amplitude or phase to represent a sequence of ones and zeros. Usually, the modulation takes the form of a square wave pattern, where each bit of information occupies one available time-slot. For such square-wave modulation the corresponding signal spectrum has the characteristic sinc shape, centered at the optical carrier

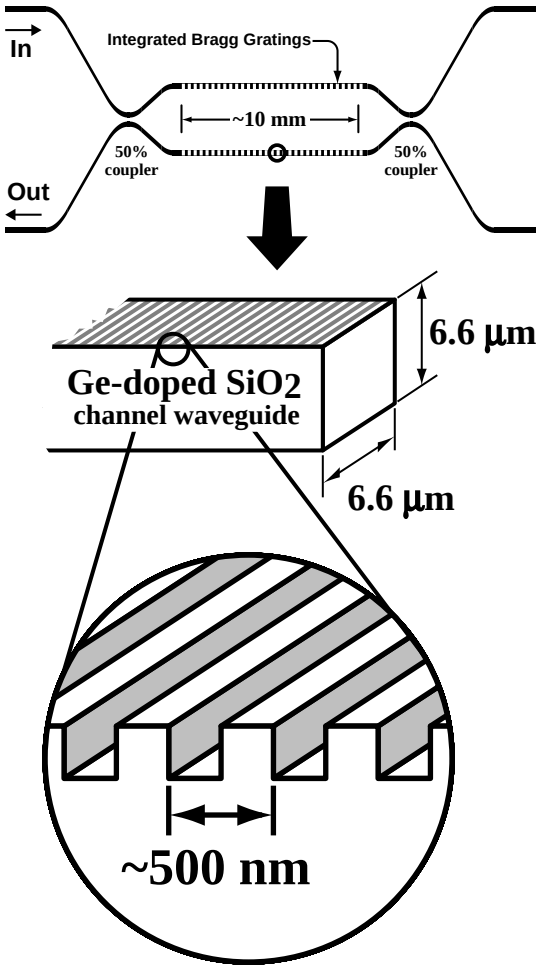

Fig. 13: Schematic of an integrated optical matched-filter. The waveguide consists of a germanium-doped SiO_2 core, 6.6 μm wide and tall, surrounded by SiO_2 cladding. The 10 mm-long Bragg grating is formed by etching a shallow, 535 nm-period grating onto the top of the waveguide before the upper cladding layer is deposited. The waveguide interferometer is designed to redirect the reflected filtered signal to a separate output port.

continued

continued

wavelength. The integrated Bragg-grating is an ideal filter for such a communications signal, because if the length and shape of the grating are properly selected, the reflection spectral response can be made to *also* have a characteristic sinc shape, matched to the binary communications signal.

Figure 13 illustrates the structure of the integrated matched-filter. The grating is formed by etching a relatively shallow corrugation onto the top surface of the waveguide structure. The length and shape of the grating are selected so that the reflection spectral response is precisely matched to a 10 Gb/s optical signal. In order to separate the reflected filtered signal from the incident noisy input signal, a Mach-Zehnder interferometer configuration is used. A noisy communication signal is launched into the upper port of the device and a codirectional coupler splits the input signal between the upper and lower arms of the interferometer. A portion of the incident light is reflected by identical Bragg gratings in the two arms of the interferometer. The reflected signals are recombined in the coupling region and emerge in the lower port of the device.

The device depicted in Figure 13 can be extended to perform other filtering functions needed in optical communications. By merely changing the properties of the Bragg grating such as the shape, period, and length, the spectral response can be tailored to suit alternative needs.

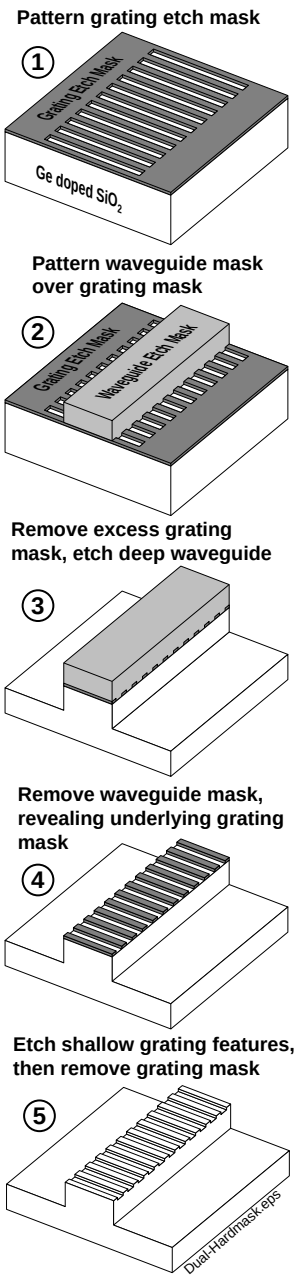

Fig. 14: (right) Fabrication sequence used to etch gratings into tall waveguides. This sequence enables both high-resolution and low-resolution lithography steps to be performed over essentially planar surfaces. The only requirement is to find two compatible etch-mask materials that can be selectively removed in subsequent steps.

continued

The fabrication of integrated grating devices presents many fabrication challenges. We have developed a flexible and robust method of constructing integrated Bragg-grating-based devices which solves some of the critical problems of alignment, period selection and grating fidelity.

While conventional photolithography is used to pattern the waveguide features of the device, patterning the fine-period grating structures requires high-resolution nanolithography techniques. We employ interferometric lithography to generate uniform, spatially-coherent gratings on X-ray masks. X-ray nanolithography is then used to transfer the grating patterns onto the substrate. We have devised an interferometric lithography system that enables us to control the grating period to within 1 nm. This is essential in order to achieve a desired center-frequency of the filter.

The integrated-matched filter requires that the sub-micron-period gratings are etched into the top surface of relatively tall (~7 μm) waveguides. To perform nanolithography over such extreme topography, we have developed a novel scheme, depicted in Figure 14 which allows all of the lithography steps to be performed over essentially planar surfaces. In this procedure, separate "hard mask" materials are used for the waveguide etch and the grating etch. The "grating" hard-mask is patterned first; then the "waveguide" hard-mask is deposited and patterned as illustrated in Figure 14. The two can be distinguished in a subsequent process step by selective chemical etching.

It is crucial to the operation of the matched filter that the arms of the interferometer be equal in optical path length. Accordingly, the Bragg grating k-vectors must be accurately aligned to the waveguide axes, e.g. within 0.2 mrad. To achieve this, we have used e-beam lithography to add alignment marks, 20 mm apart, to an interferometrically-patterned X-ray mask. A special procedure enables the e-beam system to ensure k-vector alignment. Complementary marks are included on the waveguide mask, thereby enabling angular alignment better than 0.2 mrad.

With this device, we hope to demonstrate an integrated optical grating-based noise filter that improves the performance of an optical receiver. Moreover, we believe the fabrication technology developed for this device can be applied to many other related active and passive grating-based devices. ❑

Growth of Bandgap-Engineered Distributed Bragg Reflectors

Personnel

L. A. Kolodziejski, R. J. Ram, G. S. Petrich, and S. G. Patterson

Sponsorship

JSEP

Semiconductor lasers are a powerful and pervasive device finding application in long haul fiber optic communications, local area networks, medicine, metrology, and basic research. Most commercial applications employ edge-emitting lasers. The need for lasers that (i) exhibit circular beam profiles (for coupling to fibers), (ii) possess the capability for forming 2-dimensional arrays, and (iii) integrate easily with electronics, has driven research on Vertical Cavity Surface Emitting Lasers (VCSELs). While edge emitters use cleaved facets to form the optical cavity, VCSELS are dependent upon growth technologies that are capable of near atomic layer precision, such as Molecular Beam Epitaxy (MBE), to form the Distributed Bragg Reflectors (DBRs) which are used as the optical cavity mirrors. Since the DBRs must not only act as optical reflectors, but also as electrical conductors, DBRs present a difficult design challenge to the successful implementation of low threshold current and voltage VCSELs. Toward this end, the current work has achieved the Gas Source MBE (GSMBE) growth of graded-interface DBRs utilizing $Al_{0.1}Ga_{0.9}As$ and $Al_{0.9}Ga_{0.1}As$ quarter wave layers with a 30 nm graded interface region between the layers.

Initially, a variety of compositional profiles were theoretically modeled to determine which would provide both achievable doping densities (in order to create flat valence bands for p-type DBRs) and acceptable reflectivity. When properly designed and executed, the undesired band bending in the valence band is exactly canceled by the space charge induced electric field due to the modulation doping within the DBR. The result is one or more orders of magnitude reduction in the series resistance introduced by the DBRs. To achieve acceptable reflection properties, the thickness of the graded interfacial regions must be minimized. A graded transition from GaAs to AlAs achieves the largest index contrast possible, but would result in an unacceptably wide graded region. Presently, the most practical graded transition is between $Al_{0.1}Ga_{0.9}As$ and $Al_{0.9}Ga_{0.1}As$. A further advantage of this compositional change results from the Al and Ga effusion cells remaining open throughout the DBR growth process, hence eliminating the growth rate transients associated with cell shutter openings and closings. Reflection high energy electron diffraction oscillations were used to experimentally determine the growth rates of GaAs and AlAs as a function of effusion cell temperature in order to calculate the necessary cell temperature profiles. Finally, the control parameters on the cell temperature controllers were adjusted to allow the grading profiles to closely match the model while minimizing over and undershoot transients.

Fifteen period DBRs have been grown with 30 nm $Al_{0.1}Ga_{0.9}As$ to $Al_{0.9}Ga_{0.1}As$ graded interfaces. Reflectivity and double crystal X-ray diffractometry measurements suggest that high quality graded interface DBRs have been realized. Currently, detailed doping calibrations are being done on bulk material. Upon completion, a modulation doped DBR will be fabricated. ❑